

# Tcl1 interacts with Atm and enhances NF- $\kappa$ B activation in hematologic malignancies

Eugenio Gaudio,<sup>1,2</sup> Riccardo Spizzo,<sup>3</sup> Francesco Paduano,<sup>2</sup> Zhenghua Luo,<sup>1</sup> Alexey Efanov,<sup>1</sup> Alexey Palamarchuk,<sup>1</sup> Amanda S. Leber,<sup>1</sup> Mohamed Kaou,<sup>1</sup> Nicola Zanesi,<sup>1</sup> Arianna Bottoni,<sup>1</sup> Stefan Costinean,<sup>1</sup> Laura Z. Rassenti,<sup>4</sup> Tatsuya Nakamura,<sup>1</sup> Thomas J. Kipps,<sup>4</sup> Rami I. Aqeilan,<sup>1,5</sup> Yuri Pekarsky,<sup>1</sup> Francesco Trapasso,<sup>1,2</sup> and Carlo M. Croce<sup>1</sup>

<sup>1</sup>Department of Molecular Immunology, Virology and Medical Genetics, The Ohio State University, Columbus, OH; <sup>2</sup>Department of Experimental and Clinical Medicine, University Magna Græcia of Catanzaro, Catanzaro, Italy; <sup>3</sup>Division of Experimental Oncology 2 Centro di Riferimento Oncologico, Aviano, Italy; <sup>4</sup>Department of Medicine, University of California at San Diego, La Jolla, CA; and <sup>5</sup>Lautenberg Center for Immunology and Cancer Research, Institute for Medical Research, Hebrew University, Jerusalem, Israel

**The T-cell leukemia/lymphoma 1 (*TCL1*) oncogene is a target of chromosomal translocations and inversions at 14q31.2, and its rearrangement in T cells causes T-cell prolymphocytic leukemias. *TCL1* dysregulation in B cells is responsible for the development of an aggressive form of chronic lymphocytic leukemia (CLL), the most common human leukemia. We have**

**investigated the mechanisms underlying the oncogenic functions of Tc1 protein using a mass spectrometry approach and have identified Atm (ataxia-telangiectasia mutated) as a candidate Tc1-interacting protein. The Tc1-Atm complex formation was validated by coimmunoprecipitation experiments. Importantly, we show that the association of Atm with Tc1 leads to**

**enhanced I $\kappa$ B $\alpha$  phosphorylation and ubiquitination and subsequent activation of the NF- $\kappa$ B pathway. Our findings reveal functional cross-talk between Atm and Tc1 and provide evidence for a novel pathway that could be targeted in leukemias and lymphomas. (*Blood*. 2012; 119(1):180-187)**

## Introduction

The T-cell leukemia/lymphoma 1 (*TCL1*) gene maps to chromosome 14q31.2 and is involved in chromosomal translocations and inversions in T-cell prolymphocytic leukemia (T-PLL). It is also dysregulated in several B-cell malignancies, including B-cell chronic lymphocytic leukemia (B-CLL) and in germ cell tumors, such as seminoma and dysgerminoma.<sup>1,2</sup> Normally, Tc1 protein is expressed in early embryos and fetal tissues, germ cells, and early T and B cells.<sup>3-5</sup> We previously showed that aggressive human CLLs overexpress Tc1<sup>6</sup> and that transgenic mice expressing *TCL1* in B cells developed an aggressive form of CLL.<sup>7,8</sup> These previous studies demonstrated that Tc1 up-regulation is critical in the pathogenesis of the aggressive form of human CLL. Tc1 is also known to be a coactivator of the Akt oncoprotein<sup>9</sup> and of the NF- $\kappa$ B transcription pathway.<sup>10</sup> Despite efforts to clarify the molecular mechanisms of Tc1 oncogenic function, the identification of specific pathways through which Tc1 modulates oncogenic functions has been elusive. This was mainly because Tc1 interacting proteins could not be identified by conventional methods aimed to isolate protein-protein complexes, with the exception of Akt, a protein unlikely to play a significant role in B-cell malignancies.<sup>10,11</sup> The *ATM* (ataxia-telangiectasia mutated) gene, located at chromosome 11q22.3,<sup>12</sup> is responsible for a rare disorder called ataxia-telangiectasia (AT), an autosomal recessive disease characterized by progressive cerebellar degeneration, variable immunodeficiency, genomic instability, and susceptibility to cancer, especially lymphoid malignancies.<sup>12-14</sup> *ATM* is thought to be a tumor suppressor gene because DNA double-strand breaks caused by ionizing radiation or chemicals result in rapid Atm autophosphory-

lation and activation, leading to checkpoint activation and phosphorylation of substrates that regulate cell-cycle progression, DNA repair, recombination, transcription, and cell death.<sup>12,15</sup>

Atm is a Ser/Thr kinase responsible for the phosphorylation of many substrates, including p53, Nbs1, Chk2, H2A.X, Mdm2, 4E-BP1, and I $\kappa$ B $\alpha$ . I $\kappa$ B $\alpha$  is an inhibitor of NF- $\kappa$ B, a transcription factor involved in a variety of hematologic and solid tumor malignancies.<sup>16</sup> I $\kappa$ B $\alpha$ <sup>17-21</sup> phosphorylation leads to its degradation followed by activation of NF- $\kappa$ B. Atm has a carboxy-terminal sequence with significant homology to the catalytic domain of phosphatidylinositol-3-OH kinase (PI3K).<sup>15</sup> AKT is a downstream target of PI3K and interacts directly with Tc1.<sup>22</sup> *ATM* biallelic loss in AT leads to chromosomal translocations and inversions at 14q31.2, resulting in Tc1 overexpression in AT patients. Preleukemic and leukemic T cells from AT patients with 14q31.2 chromosomal rearrangements have been found to overexpress *TCL1*.<sup>12,23,24</sup>

We assumed that Tc1 interacts with some proteins involved in important pathways up-regulated in hematologic malignancies. The aim of this work was to identify new partners of Tc1 and uncover its role in oncogenesis using a mass spectrometry approach.

## Methods

### DNA constructs

Human *TCL1* full-length was cloned into a pCMV5 vector to obtain both pCMV5-*TCL1* WT and pCMV5-*TCL1* WT HA-tagged vectors. The pcDNA 3.1 *ATM*-wt HIS6-FLAG-tagged and pcDNA 3.1 *ATM*-KD

Submitted August 22, 2011; accepted November 2, 2011. Prepublished online as *Blood* First Edition paper, November 7, 2011; DOI 10.1182/blood-2011-08-374561.

The online version of this article contains a data supplement.

The publication costs of this article were defrayed in part by page charge payment. Therefore, and solely to indicate this fact, this article is hereby marked "advertisement" in accordance with 18 USC section 1734.

© 2012 by The American Society of Hematology

HIS6-FLAG constructs were obtained from Dr M. B. Kastan (Department of Oncology, St Jude Children's Research Hospital, Memphis, TN).

A glutathione S-transferase (GST)-encoding DNA fragment was cloned between the Omni-tag and *TCL1* cDNA sequence of the Omni-*TCL1* construct to generate the Omni-GST-*TCL1* construct. I $\kappa$ B $\alpha$  cDNA was cloned into a pcDNA3.1-V5-His6 tag vector in frame with the tags. The Dual-luciferase Reporter Assay System and Renilla luciferase reporter vector pRL-TK were purchased from Promega. pNF- $\kappa$ B-Luc and the construct encoding the kinase domain of MEKK1 under the transcriptional control of the CMV promoter, pFC-MEKK, were purchased from Stratagene.

### Cells, transfections, and antisera

HEK-293 cells were grown in DMEM with 10% FBS and 100  $\mu$ g/L gentamicin at 37°C. FuGene 6 transfection reagent and protease inhibitor mixture tablets were purchased by Roche Diagnostics. Daudi lymphoma cells were grown in RPMI 1640 medium with 10% FBS and 100  $\mu$ g/L gentamicin at 37°C. Daudi cells and CLL samples were transfected with nucleofector following AMAXA guidelines for cells in suspension.

Immunoblots were developed using denville HyGlo ECL. Antibodies used were: anti-Tcl1 (Santa Cruz Biotechnology; sc-32331), for Western blots and immunoprecipitation, anti-Atm (Santa Cruz Biotechnology; sc-23921), resin conjugated with Atm from Bethyl (for IPs), anti-Egr1 (Santa Cruz Biotechnology, sc-189) and anti-I $\kappa$ B $\alpha$  (Cell Signaling), resin-conjugated HA (Bethyl for mass spectrometry experiments and IPs), anti-HA-HRP (Roche Diagnostics), and anti-V5 (Invitrogen for ubiquitination experiments).

### In vitro cell growth assessment

Daudi cells were seeded at  $2 \times 10^4$  cells per 60-mm diameter dish; cells were either untreated or treated with *TCL1* siRNA, Kudos, or combinations of both. Cells were monitored and counted at 24-hour intervals.

### Western blotting, immunoprecipitation analysis, and cell fractionation

Coimmunoprecipitation experiments were performed by incubating 1 mg of total lysates with resin-conjugated HA (Bethyl) or with anti-Tcl1 antibody conjugated with Sepharose beads, or with Atm-resin conjugated overnight at 4°C; after washing, beads were boiled in 1 $\times$  SDS sample buffer and proteins separated on 4% to 20% polyacrylamide gels (Bio-Rad). A kit from Biovision was used to perform protein fractionation of cytosol and nucleus. GST pull-down was done by incubating 1 mg of whole-cell extracts with GST beads with rocking overnight at 4°C. Dithiobis (succinimidylpropionate) crosslinker was from Pierce Chemical.

### RNA isolation and quantitative RT-PCR

Purification of total RNA was performed using TRIzol reagent (Invitrogen). A total of 500 ng of total RNA was used for the retrotranscription step. The 2<sup>- $\Delta$ Ct</sup> method was used to calculate the relative abundance of *EGR1* compared with *GAPDH* expression. To generate complete cDNAs for expression of proteins, 500 ng of total RNA was retrotranscribed using a high-capacity cDNA reverse transcription kit (Applied Biosystems) with random primers, according to the manufacturer's protocol. Real-time PCR analysis of the samples was carried out with SYBR Green PCR master mix (Applied Biosystems). *EGR1* and *GAPDH* primers were bought from Real-Time Primers LLC.

### Mass spectrometry studies

Protein pellets were solubilized and digested by trypsin. Protein constituents were identified by liquid chromatography tandem mass spectrometry (LC-MS/MS). Inspection of LC-MS/MS data was undertaken to assess exclusive presence of mass peaks belonging to candidate partner proteins in samples from cells transfected with tagged *TCL1*-HA.

### Digestion and MALDI analysis

Immunoprecipitated protein complexes were digested with sequencing grade trypsin from Promega using the Multiscreen Solvint Filter Plates

from Millipore. Briefly, complexes were incubated with a dithiothreitol solution (25mM in 100mM ammonium bicarbonate) for 30 minutes before the addition of 55mM iodoacetamide in 100mM ammonium bicarbonate solution. Iodoacetamide was incubated with protein complexes in the dark for 30 minutes before removal. Enzymatic digestion was carried out with trypsin (12.5 ng/ $\mu$ L) for 18 hours at 37°C. The digestion was stopped with addition of 0.5% trifluoroacetic acid. The MS analysis was immediately performed to ensure high-quality tryptic peptides with minimal nonspecific peptides.

### Mass spectrometry, LTQ

Capillary-liquid chromatography-nanospray tandem mass spectrometry (LC/MS/MS) was performed on a Thermo Finnigan LTQ mass spectrometer equipped with a nanospray source operated in positive ion mode. The LC system was an UltiMate 3000 system from Dionex. The solvent A was water containing 50mM acetic acid, and the solvent B was acetonitrile. A total of 5  $\mu$ L of each sample was first injected onto the m-Precolumn Cartridge (Dionex) and washed with 50mM acetic acid. The injector port was switched to inject, and the peptides were eluted off the trap onto the column. A 5-cm, 75-mm ID ProteoPep II C18 column (New Objective) packed directly in the nanospray tip was used for chromatographic separations. Peptides were eluted directly off the column into the LTQ system using a gradient of 2% to 80% B over 45 minutes, with a flow rate of 300 nL/min. The total run time was 65 minutes. The MS/MS was acquired according to standard conditions established in the laboratory. Briefly, a nanospray source operated with a spray voltage of 3 kV and a capillary temperature of 200°C. The scan sequence of the mass spectrometer was based on the TopTen method; the analysis was programmed for a full scan recorded between 350 and 2000 Da and an MS/MS scan to generate product ion spectra to determine amino acid sequence in consecutive instrument scans of the 10 most abundant peaks in the spectrum. The CID fragmentation energy was set to 35%. Dynamic exclusion was enabled with a repeat count of 2 within 10 seconds, a mass list size of 200, an exclusion duration 350 seconds, the low mass width was 0.5, and the high mass width was 1.5.

### Protein identification

The RAW data files collected on the mass spectrometer were converted to mzXML and MGF files by use of MassMatrix data conversion tools (Version 1.3; <http://www.massmatrix.net/download>). For low mass accuracy data, tandem MS spectra that were not derived from singly charged precursor ions were considered as both doubly and triply charged precursors. The resulting MGF files were searched using Mascot Daemon by Matrix Science Version 2.2.2, and the database searched against the full SwissProt Version 57.5 database (471 472 sequences; 167 326 533 residues) or NCBI database Version 20091013 (9 873 339 sequences; 3 367 482 728 residues). The mass accuracy of the precursor ions was set to 2.0 Da, given that the data were acquired on an ion trap mass analyzer and the fragment mass accuracy was set to 0.5 Da. Considered modifications (variable) were methionine oxidation and carbamidomethyl cysteine. Two missed cleavages for the enzyme were permitted. A decoy database was searched to determine the false discovery rate, and peptides were filtered according to the false discovery rate and proteins identified required bold red peptides. Protein identifications were checked manually, and proteins with a Mascot score of 50 or higher with a minimum of 2 unique peptides from 1 protein having a -b or -y ion sequence tag of 5 residues or better were accepted.

### Ubiquitination experiments

Total protein lysates (1 mg) were incubated overnight with V5 antibody (Invitrogen) and AG/agarose beads and then run on 4% to 20% polyacrylamide gels. The nitrocellulose membrane was immunoblotted with anti-HA-HRP to detect Ub-HA (ubiquitin), anti-I $\kappa$ B $\alpha$ , anti-Atm, and anti-Tcl1A.

### Luciferase assay

HEK-293 cells were transfected with the indicated constructs. Firefly and Renilla luciferase activities were assayed with the Dual Luciferase Assay

System (Promega), and firefly luciferase activity was normalized to Renilla luciferase activity, as suggested by the manufacturer. All experiments were carried out in triplicate and repeated 3 times with consistent results.

### Isolation of B cells

CD19<sup>+</sup> B cells were isolated from mouse spleen following the protocol and using reagents from Miltenyi Biotec (CD19 microbeads, mouse).

### Patients

B-CLL samples were obtained after informed consent in accordance with the Declaration of Helsinki from patients diagnosed with B-CLL from the CLL Research Consortium. Research was performed with the approval of the Institutional Review Board of The Ohio State University. Briefly, blood was obtained from CLL patients, and lymphocytes were isolated through Ficoll/Hypaque gradient centrifugation (GE Healthcare) and processed for protein extraction.

### Animal studies

Mice were maintained and animal experiments conducted under institutional guidelines established for the Animal Facility at The Ohio State University; nu/nu mice were obtained from The Jackson Laboratory. Tumors were established by injecting Daudi lymphoma cells (200  $\mu$ L PBS,  $7.5 \times 10^7$  cells/mouse) into the right flanks of female nude mice at 6 weeks of age (Charles River Breeding Laboratories). Tumor size was measured daily until tumors reached 50 mm<sup>3</sup>. Then, 5  $\mu$ g of synthetic siRNA for Tc11 or scrambled siRNA (si-Scr) diluted in Lipofectamine and w/o Kudos 55933 (Atm inhibitor) in combination (50  $\mu$ L total volume) were injected directly into the tumors and after 3, 7, and 10 days. Tumors were measured on the day of the injections and 4 days after the last injection. At that time, the mice were killed and tumors were weighed. Tumor volumes were calculated using the equation  $V$  (in mm<sup>3</sup>) =  $A \times B^2/2$ , where A is the largest diameter and B is the perpendicular diameter.

### Statistics

All graph values represent the mean  $\pm$  SEM from 3 independent experiments with each measured in triplicate. The differences between 2 groups were analyzed with unpaired 2-tailed Student *t* test.  $P < .05$  was considered statistically significant and indicated with asterisks as described in the figure legends.

## Results

### Tc11 interacts with Atm and both affect I $\kappa$ B $\alpha$ expression

To identify Tc11-interacting proteins, we used a *TCL1* cDNA modified at its 3' end with a sequence encoding a HA tag (*TCL1*-HA). A549 lung cancer-derived cells, used as recipient, were transfected either with wild-type *TCL1* (used as a control) or *TCL1*-HA and treated with dithiobis (succinimidylpropionate), a cross-linker that fixes protein complexes in vivo. We used A549 cells in our experiment because no CLL cell lines are currently available; furthermore, these cells can be easily transfected at a very high efficiency, an important requirement for such an experiment.

Cells were lysed; and Tc11-HA protein, along with candidate protein partners, was isolated using a HA-conjugated resin. Purified proteins were treated with dithiothreitol to cleave dithiobis (succinimidylpropionate) and dissociate complexes, and digested by trypsin; protein constituents were identified by LC-MS/MS (supplemental Table 1, available on the *Blood* Web site; see the Supplemental Materials link at the top of the online article). Among the identified candidate interactors, we focused on Atm because its role in leukemogenesis has been already assessed.<sup>13</sup>

The potential interaction between Tc11 and Atm proteins was investigated using coimmunoprecipitation experiments. HEK293 cells were stably transfected with a FLAG-*ATM* construct and infected with a recombinant Adeno-*TCL1*. Infected cell lysates were immunoprecipitated with Atm antisera, followed by immunoblotting with both Tc11 and Atm antisera. As shown in Figure 1A (bottom panel lane 3), Tc11 interacts with Atm; no Tc11 protein was detected in anti-IgG immunoprecipitates (Figure 1A lane 2). The same complexes were detected in the reverse experiment, where cell lysates were immunoprecipitated with anti-Tc11 and probed with both Atm and Tc11 antisera (Figure 1B).

Because DNA-damaging agents cause Atm phosphorylation, we investigated whether such treatment could affect the Tc11-Atm interaction. HEK293 cells were cotransfected with FLAG-*ATM* and Omni-GST-*TCL1* plasmids and treated with neocarzinostatin and double-strand breaks.<sup>25</sup> Tc11 binds Atm with higher affinity after treatment with the DNA-damaging agent, whereas protein complexes with Omni-GST-*FHIT* protein, used as a negative control, were not detected (Figure 1C). The interaction was also validated with endogenous proteins. The results also indicated (Figure 1C) that Tc11 has a higher affinity for activated Atm. The structural basis for this phenomenon will require further investigation. Tc11 and Atm were immunoprecipitated and immunoblotted in Daudi lymphoma cells with or without the DNA-damaging agent (Figure 1D-E). To understand the functional relevance of the Tc11-Atm interaction, we analyzed the phosphorylation status of several Atm substrates in the presence of Tc11. Interestingly, we detected an increase of Atm-mediated I $\kappa$ B $\alpha$  phosphorylation in the presence of Tc11 (Figure 1F). Because Atm-mediated phosphorylation of I $\kappa$ B $\alpha$  enhances its degradation, we examined the expression level of I $\kappa$ B $\alpha$  after Tc11 and Atm coexpression. DNA double-strand breaks induced by hydroxyurea are responsible for Atm activation.<sup>26</sup> HEK293 cells were mock-transfected or transfected with *TCL1* and *ATM* constructs, separately or together (Figure 1F-G). Forty-eight hours later, cells were treated with hydroxyurea for 3 hours and cell lysates were analyzed by Western blotting. We found that Tc11 and Atm coexpression was associated with increased levels of the phosphorylated form of I $\kappa$ B $\alpha$  and reduced levels of total I $\kappa$ B $\alpha$  (Figure 1F). Figure 1G shows an increased ratio of phosphorylated I $\kappa$ B $\alpha$  (Ser 32) relative to total I $\kappa$ B $\alpha$ . Daudi lymphoma cells were treated with siRNA for Tc11, Kudos 55933 (an Atm inhibitor), and a combination of both; both I $\kappa$ B $\alpha$  expression and its phosphorylation were measured (Figure 1H-I). Taken together, these data indicate that the interaction of endogenous Tc11 and Atm is responsible for an increase in phosphorylation and degradation of I $\kappa$ B $\alpha$  and in activation of NF- $\kappa$ B, whereas inhibition of Tc11 and Atm resulted in decreased activity of the NF- $\kappa$ B pathway.

### Expression of Tc11 and Atm activates the NF- $\kappa$ B pathway

I $\kappa$ B $\alpha$  is phosphorylated by Atm, leading to its ubiquitination and degradation.<sup>17,19,27</sup> To determine whether Tc11 expression affects I $\kappa$ B $\alpha$  regulation through Atm, we carried out a ubiquitination assay. HEK293 cells were transfected with *TCL1*, *ATM*, *Ub-HA*, and *I $\kappa$ B $\alpha$ -V5* expression vectors (Figure 2A). Forty-eight hours after transfection, cells were treated with MG132, a proteasome inhibitor, 10  $\mu$ M for additional 3 hours, then lysed and protein immunoprecipitated with anti-V5 followed by immunoblotting with anti-HA. Coexpression of Tc11 and Atm resulted in I $\kappa$ B $\alpha$  ubiquitination (Figure 2A lane 1), whereas expression of Atm or Tc11 alone did not (Figure 2A lanes 2 and 3). These results suggest that Tc11 expression enhances Atm-mediated phosphorylation and ubiquitination of I $\kappa$ B $\alpha$ . Because ubiquitination of I $\kappa$ B $\alpha$  is

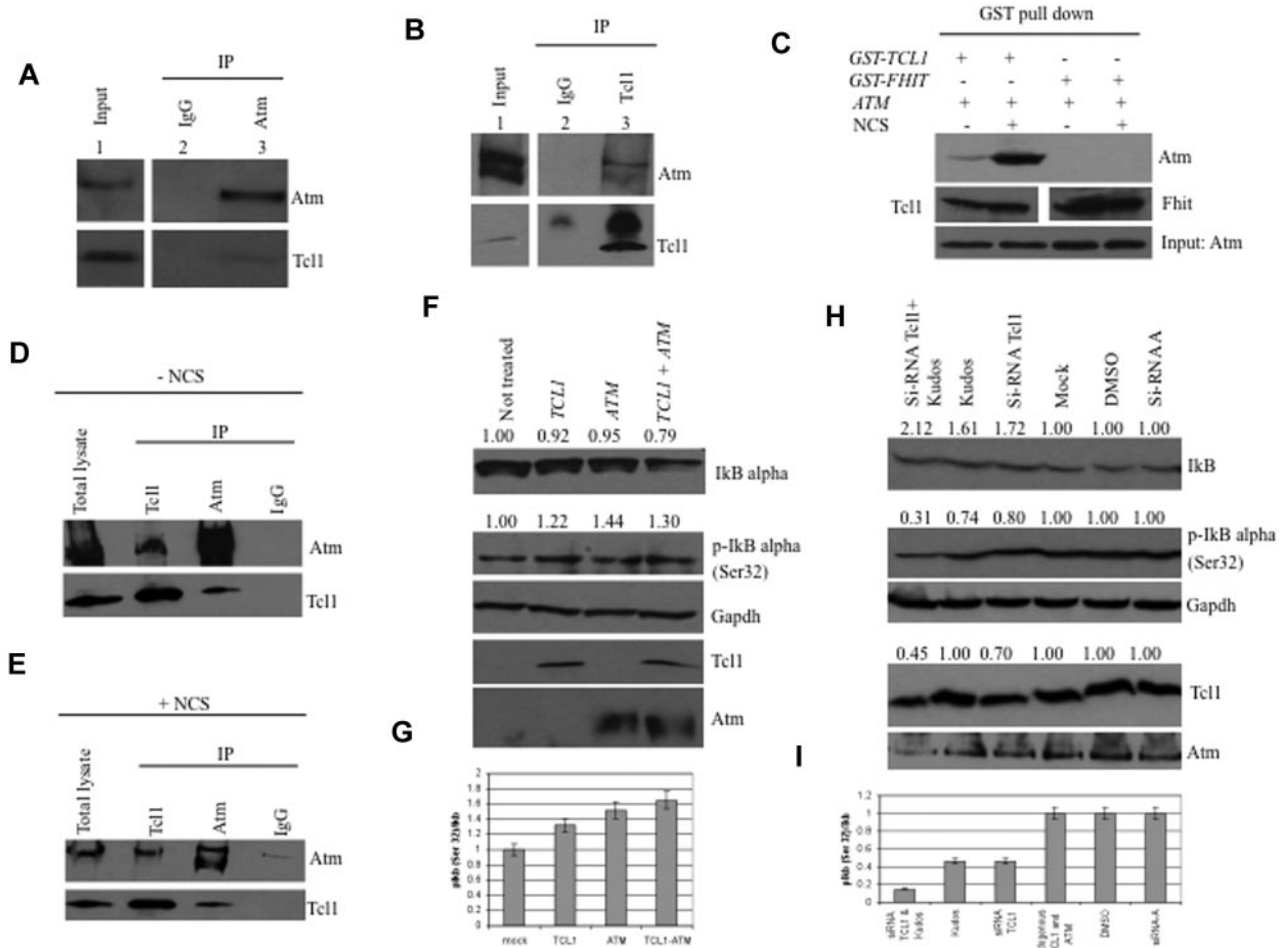


**Figure 1. Tc1l interacts with Atm, and both affect IκBα expression.** (A) HEK293 cells were stably transfected with expression plasmid encoding FLAG-ATM and then infected with Ad-TCL1 wild-type (MOI 100). Forty-eight hours after infection, whole-cell lysates were immunoprecipitated with anti-Atm (resin conjugated to Atm). The immunoprecipitates were analyzed by Western blot with anti-Atm or anti-Tc1l. Input: lysate expression of Atm (top) and Tc1l (bottom). (B) HEK293 cells were transiently cotransfected with expression plasmids encoding mammalian FLAG-ATM (8 μg) and wild-type TCL1 (6 μg). Forty-eight hours after transfection, cell lysates were immunoprecipitated with anti-TCL1. The immunoprecipitates were analyzed by Western blot with anti-Atm or anti-Tc1l. Input: lysate expression of Atm (top) and Tc1l (bottom). (C) HEK293 cells were transiently cotransfected with expression plasmids encoding mammalian Omni-GST-TCL1 (6 μg) or Omni-GST-FHIT (6 μg) and FLAG-HIS-ATM (8 μg). Forty-eight hours after transfection, cells were treated with neocarzinostatin (NCS) 200 ng/mL for 2 hours. Cell lysates were GST-pulled down and immunoblotted with anti-His6, anti-Tc1l, and anti-Fhit. Input: lysate expression of Atm. (D-E) Daudi cells were untreated or treated with hydroxyurea, 50mM for 3 hours, then lysed and immunoprecipitated with anti-TCL1. The immunoprecipitates were analyzed by Western blot with anti-Atm or anti-Tc1l. (F) Tc1l and Atm coexpression is associated with decreased IκBα total protein. HEK293 cells were mock-transfected or transfected with TCL1 or ATM plasmids separately or together (4 μg for each plasmid, including empty vector). Forty-eight hours later, cells were treated with hydroxyurea 50mM for 3 hours and then analyzed by Western blot with the indicated antibodies. (G) Tc1l and Atm coexpression is associated with increased IκBα (Ser32) phosphorylation as shown in the graph. (H) Daudi cells were mock-transfected or transfected with si-TCL1 or si-Scr, and then untreated or treated with Kudos 55933 or DMSO. The level of IκBα was measured by Western blot. (I) IκBα (Ser 32) levels are shown in the graph. Data are representative of 3 independent experiments.

associated with NF-κB activation and translocation from the cytosol to nucleus,<sup>20,21,28</sup> we investigated whether active p65 NF-κB (Rel-A) translocates from the cytosol to the nucleus when *TCL1* and *ATM* are coexpressed (Figure 2B). To this end, HEK293 cells were transfected with *ATM* and *TCL1* constructs, separately or together; then, cell lysates were fractionated to obtain nuclear and cytosolic fractions and the fractions run on gels. The level of nuclear Rel-A increased when *TCL1* and *ATM* were coexpressed (Figure 2B). Expression of Rel-A was compared with Gapdh and H2A (histone 2A) expression, as markers for cytosol and nucleus, respectively. These results suggest that Tc1l and Atm coexpression is associated with Rel-A translocation into the nucleus. After its translocation into the nucleus, Rel-A enhances the transcription of several target genes, including *EGR1* (early growth response 1); indeed, Rel-A binds *EGR1* promoter sequences and enhances *EGR1* mRNA and protein expression.<sup>29</sup> Thus, we determined whether *TCL1* expression could modulate this Rel-A function. HEK293 cells were transfected with *TCL1* and *ATM* separately or together and

treated with hydroxyurea for 3 hours and protein lysates fractionated on gels. Egr1 protein levels were increased when Tc1l and Atm were coexpressed (Figure 2D middle panel). *EGR1* mRNA expression measured by quantitative RT-PCR was also increased during coexpression of *TCL1* and *ATM* (Figure 2C). To determine whether Tc1l expression directly affects the transactivating function of NF-κB, we used a commercial system based on the ability of mitogen-activated protein kinase kinase 1 (MEKK1) to activate an NF-κB reporter construct, pNF-κB-Luc expressing luciferase under the control of an NF-κB-responsive element. Expression of *ATM* alone did not affect the reporter activity. Interestingly, Tc1l by itself increased reporter activity by 2.5-fold (Figure 2E). When coexpressed, the Tc1l-Atm complex enhanced the NF-κB transactivating function approximately 4-fold (Figure 2E). To confirm that Tc1l and Atm are equally important in NF-κB activation, we treated cells with Kudos 55933, an inhibitor of endogenous and exogenous Atm. Kudos inhibited NF-κB activation by Tc1l or by Tc1l plus Atm (Figure 2E right), suggesting that this function

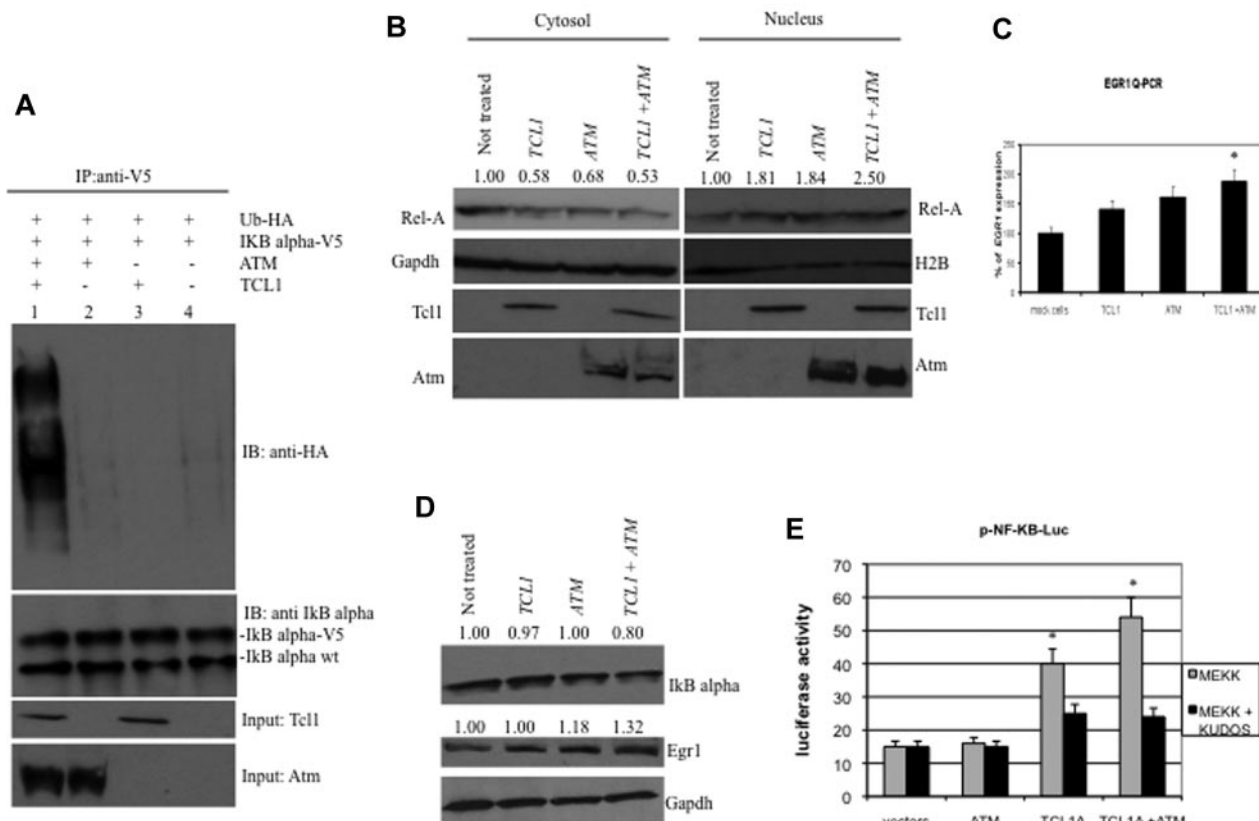


**Figure 2. Expression of Tc1 and Atm activates the NF- $\kappa$ B pathway.** (A) HEK293 cells were transfected with indicated plasmids. Forty-eight hours later, cells were treated with MG132, 10 $\mu$ M for 3 hours, and then lysates immunoprecipitated with anti-V5. The precipitates were analyzed by Western blot with anti-HA or anti-I $\kappa$ B $\alpha$ . Input: lysate expression of Tc1 and Atm. (B) HEK293 cells were mock-transfected or transfected with *TCL1* and *ATM* plasmids separately or together (4  $\mu$ g each plasmid). Forty-eight hours later, cells were treated with hydroxyurea for 3 hours, fractionated into cytosolic and nuclear fractions, and analyzed by Western blot with the indicated antibodies. (C) mRNA levels of *EGR1* were measured by quantitative RT-PCR. HEK293 cells were mock-transfected or transfected with *TCL1* and *ATM* plasmids, separately or together for 48 hours, and then treated with hydroxyurea, 50mM for 3 hours). Fold changes of *EGR1* were calculated using the  $2^{-\Delta\Delta Ct}$  method. GAPDH mRNA levels were used as an internal normalization control. Samples transfected with *TCL1* and *ATM* have been normalized to mock-transfected sample. (D) HEK293 cells were transfected with *TCL1* and *ATM* (4  $\mu$ g for each plasmid), treated with hydroxyurea for 3 hours and with MG132, 10 $\mu$ M 6 hours, and protein lysates run on gel. (E) Tc1 activates NF- $\kappa$ B-dependent transcription synergistically with Atm. HEK-293 cells were cotransfected with 50 ng of pNF- $\kappa$ B-Luc reporter and 50 ng of pRL-TK *Renilla* reporter constructs. In addition, 0.75  $\mu$ g of CMV5-empty vector, 0.75  $\mu$ g of pcDNA 3.1 empty vector, 0.75  $\mu$ g of CMV5-*TCL1* WT, and 0.75  $\mu$ g of pcDNA 3.1 empty vector constructs were used; 5 ng of pFC-MEKK was added where indicated. Cells were treated with 10 $\mu$ M Kudos for 5 hours, where indicated. Data are representative of 3 independent experiments. (C,E) Data are mean  $\pm$  SEM of 3 independent experiments, and each is measured in triplicate. \* $P < .05$ .

of Tc1 is enhanced by endogenous as well as exogenous Atm. In summary, these results suggest that Tc1 and Atm cooperate to induce NF- $\kappa$ B activation.

#### Tc1 and Atm are crucial for proliferation in vitro and in vivo

We investigated the role of Tc1 depletion on the proliferation of Daudi lymphoma cells, which express both Tc1 and Atm. The combination of Kudos 55933 treatment with Tc1 depletion had an additive effect on cell proliferation (Figure 3A). Effects on proliferation were not observed after transfection with the carrier alone or scrambled siRNAs. The data reported represent the mean (SD) values of 3 different experiments (Figure 3A). Tc1 protein expression was silenced with siRNAs. In Figure 3B, the effects of specific Tc1-siRNA on Tc1 protein expression levels are shown. Daudi cells were transfected with Tc1-siRNAs in the absence or presence of Kudos 55933; in lanes 1 and 3, Tc1 protein expression is down-regulated by Tc1 siRNA. No effects on Tc1 expression level were detected after scrambled siRNA transfection (lane 6). Total proteins extracted from Daudi cells, 5 days after transfection, were analyzed by immunoblotting (Figure 3B). The expression of Tc1 was affected by Tc1 siRNA; and more importantly, PARP was cleaved in the condition of depleted Tc1 and Kudos inhibition of

Atm. Finally, we investigated the effects of Tc1 depletion by siTc1 and Kudos 55933 treatment in vivo in a preclinical model of lymphoma; 5 groups of 4 mice each were injected with Daudi cells (Figure 3C). Xenograft tumors treated with Kudos 55933 or Tc1 siRNA separately showed a reduction in volume compared with controls. A dramatic effect on inhibition of tumor growth was observed in the group of mice treated with Kudos 55933 and Tc1 siRNA in combination. Total proteins extracted from tumors were analyzed by Western blotting, and Tc1 expression was measured (Figure 3D). At the end of the experiment, tumors were excised and weighed (Figure 3E). These in vivo data confirmed the in vitro results and illustrated the effect of Atm and Tc1 cross-talk.

#### Tc1 and Atm affect the NF- $\kappa$ B pathway in CLL samples and transgenic Tc1 mice

To investigate whether our results are relevant to human CLL, we studied the expression of I $\kappa$ B $\alpha$  and Egr1 in human CLL samples (Figure 4A). CLL samples (supplemental Table 2) were transfected with Tc1 siRNA for 36 hours and/or treated with Kudos (10 $\mu$ M, 12 hours; Figure 4A). Mock-treated samples showed low expression of I $\kappa$ B $\alpha$  and high expression of Egr1. CLL samples treated either with Tc1 siRNA or Kudos or both showed increased I $\kappa$ B $\alpha$  expression and decreased

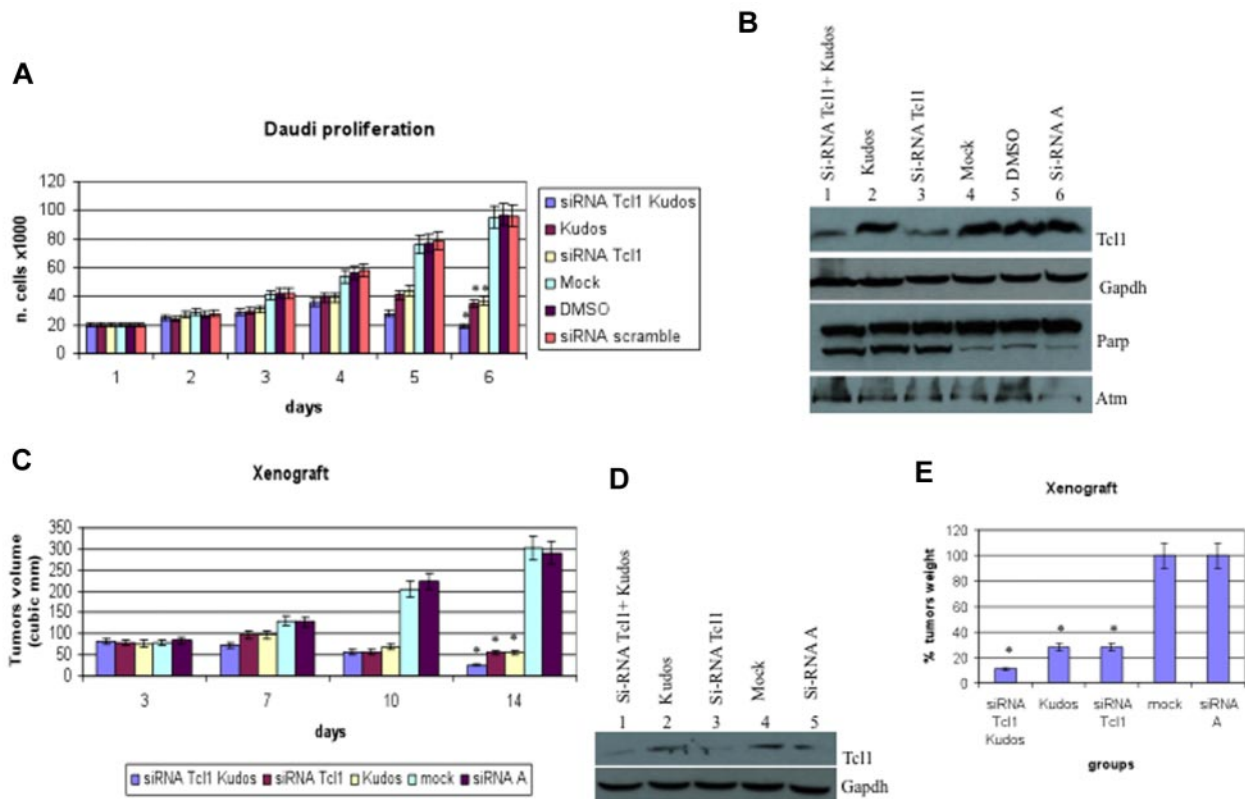


**Figure 3.** Tcl1 and Atm are crucial for growth and proliferation of lymphoma cells in vitro and in vivo. (A) Daudi cells were mock-transfected or transfected with si-TCL1 or si-Scr and then untreated or treated with Kudos 55933 or DMSO. Cells were counted at 24-hour intervals. Results represent the average of 3 independent experiments. (B) Total lysates collected were analyzed by Western blot and tested with indicated antibodies. (C) Graph representing tumor volumes at indicated days during the experiment for the 5 groups indicated (4 mice/group). Tumor size was measured daily until the tumor reached 50 mm<sup>3</sup>. Then, 5  $\mu$ g of synthetic si-TCL1 or si-Scr diluted in Lipofectamine and with or without Kudos (50  $\mu$ L total volume) were injected directly into the tumors and at 3, 7, and 10 days. Tumors were measured on the day of the injections and 4 days after the last injection. (D) Total lysates from tumors were analyzed by Western blot and tested with indicated antibodies. (E) Xenograft tumors were weighed. Data are mean  $\pm$  SEM of 3 independent experiments, and each is measured in triplicate. \* $P$  < .05.

expression of Egr1 compared with the mock-treated control. These data confirmed cooperation of Tcl1 and Atm in NF- $\kappa$ B activation in CLL. In addition, we were able to confirm the interaction between endogenous Tcl1 and Atm in some B-CLL patient samples. B-CLLs were lysates and immunoprecipitated with anti-Tcl1 antibody; the immunoblotting with anti-Atm antibody confirmed the interaction (Figure 4C).

We also show evidence of NF- $\kappa$ B pathway activation in transgenic Tcl1 mice. A transgenic mouse model of CLL was generated by introducing the human *TCL1* gene under control of a B cell-specific IgE $\mu$  enhancer.<sup>7,30</sup> Overexpression of Tcl1 in these mice resulted in up-regulation of Atm and down-regulation of I $\kappa$ B $\alpha$  (Figure 4B). TCL1 transgenic mice develop monoclonal B-cell leukemia that is very similar to the aggressive form of human CLL. We isolated CD19<sup>+</sup> B cells from spleens of Tcl1 transgenic and wild-type mice. We found that Tcl1 expression is associated with overexpression of Atm and down-regulation of I $\kappa$ B $\alpha$  in Tcl1 transgenic CD19<sup>+</sup> B cells compared with wild-type CD19<sup>+</sup> B cells used as a control (Figure 4B).

## Discussion

Dysregulation of *TCL1* in T and B cells causes T-cell prolymphocytic leukemias<sup>3,31</sup> and the aggressive form of CLL,<sup>7,8</sup> respectively. To clarify the function of Tcl1 in leukemia, we studied Tcl1 protein complexes using a proteomic approach. Atm was identified as a

candidate Tcl1 partner, and the interaction was confirmed by coimmunoprecipitation experiments. Atm may act as an upstream kinase that mediates the constitutive NF- $\kappa$ B activation in marrow blasts in both high-risk myelodysplastic syndrome and acute myeloid leukemia.<sup>18</sup> The analysis of the phosphorylation status of Atm substrate proteins directed our experiments toward the study of the NF- $\kappa$ B pathway. We previously demonstrated that Tcl1 is responsible for the activation of NF- $\kappa$ B,<sup>10</sup> although that study did not show the mechanisms of such an activation. Here we propose the following mechanism based on the previous paragraph: through interacting with Atm, Tcl1 expression causes an increase in Atm kinase activity, an increase in phosphorylation of I $\kappa$ B $\alpha$ , and translocation Rel-A to the nucleus; Tcl1 and Atm have a common target: I $\kappa$ B $\alpha$ , a physiologic NF- $\kappa$ B inhibitor. Indeed, Tcl1 interacts with I $\kappa$ B $\alpha$ ,<sup>32</sup> whereas Atm phosphorylates it,<sup>17,18</sup> which is subsequently degraded by ubiquitination.<sup>28</sup>

Because Tcl1 interacts with both I $\kappa$ B $\alpha$  and Atm, we detected an additive effect on I $\kappa$ B $\alpha$  ubiquitination when Tcl1 and Atm are coexpressed. As a result of degradation of I $\kappa$ B $\alpha$ , p65 NF- $\kappa$ B active (Rel-A) translocates from the cytosol to the nucleus. Rel-A interacts with the *EGR1* promoter sequence and causes overexpression of Egr1 protein,<sup>29</sup> as detected by Western blot and quantitative PCR. To confirm that our findings are relevant to human CLL, B-CLL samples were treated with *TCL1* siRNA, Kudos, or both to reduce the expression/activity of Tcl1, Atm, or both proteins. Mock-treated samples, with endogenous expression of Atm and

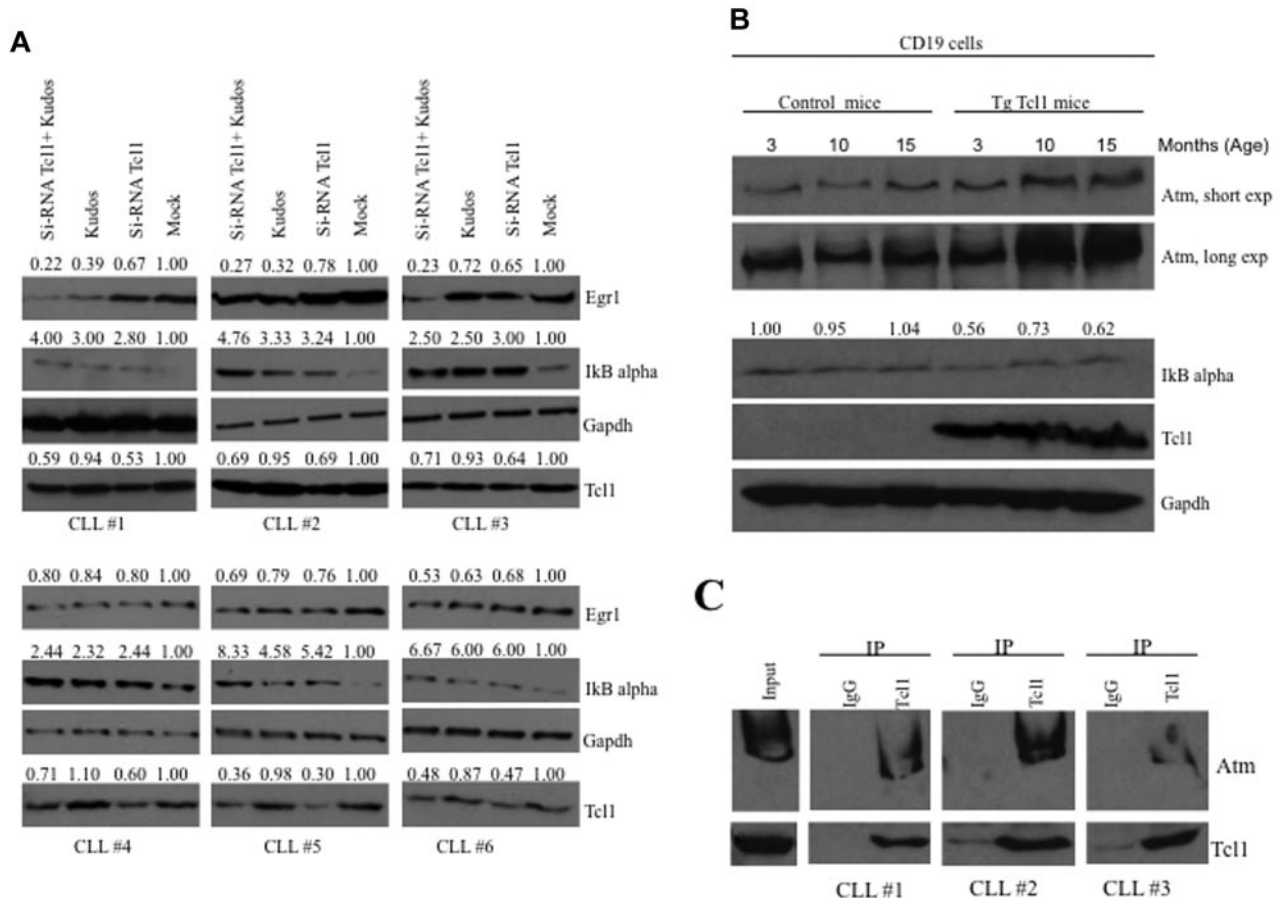


**Figure 4.** Tc1 and Atm affect the NF- $\kappa$ B pathway in CLL patient samples and Tc1 transgenic mice. (A) B-CLL samples were transfected with si-*TCL1* for 36 hours or treated with Kudos (10  $\mu$ M, 12 hours) or both and in all cases treated with hydroxyurea, 50mM 3 hours. I $\kappa$ B $\alpha$  and Egr1 expression was detected by Western blot. (B) B-cell CD19 isolated from mouse spleen was lysed and analyzed by Western blot with indicated antibodies. Splens were excised from wild-type and Tc1 transgenic mice at 3, 10, and 15 months of age. Data are representative of 3 independent experiments. (C) Whole B-CLL cell lysates were immunoprecipitated with anti-Tc1 antibody. The immunoprecipitates were analyzed by immunoblotting (IB) with anti-Atm and anti-Tc1 antibodies. Input: total lysate.

Tc1, showed significant down-regulation of I $\kappa$ B $\alpha$  and overexpression of Egr1, confirming in B cells the data obtained with transfected HEK293 cells. The NF- $\kappa$ B pathway is down-regulated in Daudi Burkitt lymphoma cells when endogenous Tc1 and Atm are targeted with si-TCL1 and Kudos 55933, both in vitro (proliferation) and in vivo (xenograft experiment). We also provided evidence of NF- $\kappa$ B pathway activation in Tc1 transgenic mice. Overexpression of Tc1 in these mice resulted in up-regulation of Atm and down-regulation of I $\kappa$ B $\alpha$ . Thus, we have shown cooperation of Tc1 and Atm in NF- $\kappa$ B activation. Our results provide additional evidence of the role of the NF- $\kappa$ B pathway in CLL. Because Atm inhibitors are able to kill malignant cells by inhibiting upstream kinases that account for constitutive activation of the NF- $\kappa$ B pathway,<sup>17</sup> our data suggest that members of the NF- $\kappa$ B pathway, as well as Tc1 and Atm interaction, could be considered targets for novel therapies for CLL.

## Acknowledgments

The authors thank Dr M. B. Kastan for the pcDNA 3.1 *ATM*-wt HIS6-FLAG tagged and pcDNA 3.1 *ATM*-KD HIS6-FLAG constructs, Dr Kari Green-Church (Mass Spectrometry and Proteomics Facility, The Ohio State University) for the mass spectrometry analysis, Grace A. Hill (Molecular Virology, Immunology and Medical Genetics, The Ohio State University Medical Center) for the assistance with animal experi-

ments, and Dr K. Huebner (Molecular Virology, Immunology, and Medical Genetics, The Ohio State University Medical Center) for the critical editing of the manuscript.

This work was supported by the American Cancer Society (Research Scholar Grant, Y.P.) and National Institutes of Health (grant PO1-CA81534 of the CLL Research Consortium, L.Z.R., T.J.K., and C.M.C.).

This work is dedicated to the memory of Pietro Gaudio, Geometra, who died on March 11, 1996.

## Authorship

Contribution: E.G., F.T., and C.M.C. designed the experiments; E.G., R.S., Z.L., F.P., M.K., A.S.L., N.Z., A.B., and S.C. performed research experiments; A.E., A.P., T.N., L.Z.R., and T.J.K. contributed new reagents; E.G., R.S., Y.P., R.I.A., F.T., and C.M.C. wrote the paper; and all authors critically reviewed the manuscript and approved the final version.

Conflict-of-interest disclosure: The authors declare no competing financial interests.

Correspondence: Carlo M. Croce, Department of Molecular Virology, Immunology, and Medical Genetics and Comprehensive Cancer Center, The Ohio State University, 1082 Biomedical Research Tower, 460 West 12th Ave, Columbus, OH 43210; e-mail: carlo.croce@osumc.edu.

## References

- Pekarsky Y, Halas C, Isobe M, Russo G, Croce CM. Abnormalities at 14q32.1 in T cell malignancies involve two oncogenes. *Proc Natl Acad Sci U S A*. 1999;96(6):2949-2951.
- Narducci MG, Fiorenza MT, Kang SM, et al. TCL1 participates in early embryonic development and is overexpressed in human seminomas. *Proc Natl Acad Sci U S A*. 2002;99(18):11712-11717.
- Virgilio L, Narducci MG, Isobe M, et al. Identification of the *TCL1* gene involved in T-cell malignancies. *Proc Natl Acad Sci U S A*. 1994;91(26):12530-12534.
- Madani A, Choukroun V, Soulier J, et al. Expression of p13MTC1 is restricted to mature T-cell proliferations with t(X;14) translocations. *Blood*. 1996;87(5):1923-1927.
- Narducci MG, Virgilio L, Engiles JB, et al. The murine *Tcl1* oncogene: embryonic and lymphoid cell expression. *Oncogene*. 1997;15(8):919-926.
- Pekarsky Y, Santanam U, Cimmino A, et al. Tcl1 expression in chronic lymphocytic leukemia is regulated by miR-29 and miR-181. *Cancer Res*. 2006;66(24):11590-11593.
- Bichi R, Shinton SA, Martin ES, et al. Human chronic lymphocytic leukemia modeled in mouse by targeted *TCL1* expression. *Proc Natl Acad Sci U S A*. 2002;99(10):6955-6960.
- Yan XJ, Albesiano E, Zanesi N, et al. B cell receptors in *TCL1* transgenic mice resemble those of aggressive, treatment-resistant human chronic lymphocytic leukemia. *Proc Natl Acad Sci U S A*. 2006;103(31):11713-11718.
- Pekarsky Y, Koval A, Hallas C, et al. Tcl1 enhances Akt kinase activity and mediates its nuclear translocation. *Proc Natl Acad Sci U S A*. 2000;97(7):3028-3033.
- Pekarsky Y, Palamarchuk A, Maximov V, et al. Tcl1 functions as a transcriptional regulator and is directly involved in the pathogenesis of CLL. *Proc Natl Acad Sci U S A*. 2008;105(50):19643-19648.
- Hofbauer SW, Pinon JD, Brachtl G, et al. Modifying akt signaling in B-cell chronic lymphocytic leukemia cells. *Cancer Res*. 2010;70(18):7336-7344.
- Shiloh Y. ATM and related protein kinases: safeguarding genome integrity. *Nat Rev Cancer*. 2003;3(3):155-168.
- Sherman MH, Kuraishy AL, Deshpande C, et al. AID-induced genotoxic stress promotes B cell differentiation in the germinal center via ATM and LKB1 signaling. *Mol Cell*. 2010;39(6):873-885.
- Gabellini C, Antonelli A, Petrinelli P, et al. Telomerase activity, apoptosis and cell cycle progression in ataxia telangiectasia lymphocytes expressing *TCL1*. *Br J Cancer*. 2003;89(6):1091-1095.
- Kastan MB, Lim DS. The many substrates and functions of ATM. *Nat Rev Mol Cell Biol*. 2000;1(3):179-186.
- Kim HJ, Hawke N, Baldwin AS. NF- $\kappa$ B and IKK as therapeutic targets in cancer. *Cell Death Differ*. 2006;13(5):738-747.
- Jung M, Kondratyev A, Lee SA, Dimtchev A, Dritschilo A. ATM gene product phosphorylates I $\kappa$ B- $\alpha$ . *Cancer Res*. 1997;57(1):24-27.
- Grosjean-Raillard J, Tailler M, Ades L, et al. ATM mediates constitutive NF- $\kappa$ B activation in high-risk myelodysplastic syndrome and acute myeloid leukemia. *Oncogene*. 2009;28(8):1099-1109.
- Wu ZH, Shi Y, Tibbetts RS, Miyamoto S. Molecular linkage between the kinase ATM and NF- $\kappa$ B signaling in response to genotoxic stimuli. *Science*. 2006;311(5764):1141-1146.
- Rosato RR, Kolla SS, Hock SK, et al. Histone deacetylase inhibitors activate NF- $\kappa$ B in human leukemia cells through an ATM/NEMO-related pathway. *J Biol Chem*. 2010;285(13):10064-10077.
- Hayden MS, Ghosh S. Shared principles in NF- $\kappa$ B signaling. *Cell*. 2008;132(3):344-362.
- Laine J, Kunstle G, Obata T, Sha M, Noguchi M. The protooncogene *TCL1* is an Akt kinase coactivator. *Mol Cell*. 2000;6(2):395-407.
- Narducci MG, Virgilio L, Isobe M, et al. *TCL1* oncogene activation in preleukemic T cells from a case of ataxia-telangiectasia. *Blood*. 1995;86(6):2358-2364.
- Thick J, Metcalfe JA, Mak YF, et al. Expression of either the *TCL1* oncogenes, or transcripts from its homologue *MTCP1/c6.1B*, in leukemic and non-leukemic T cells from ataxia telangiectasia patients. *Oncogene*. 1996;12(2):379-386.
- Dedon PC, Jiang ZW, Goldberg IH. Neocarzinostatin-mediated DNA damage in a model AGT.ACT site: mechanistic studies of thiol-sensitive partitioning of C4' DNA damage products. *Biochemistry*. 1992;31(7):1917-1927.
- Tanaka T, Huang X, Halicka HD, et al. Cytometry of ATM activation and histone H2AX phosphorylation to estimate extent of DNA damage induced by exogenous agents. *Cytometry A*. 2007;71(9):648-661.
- Kunstle G, Laine J, Pierron G, et al. Identification of Akt association and oligomerization domains of the Akt kinase coactivator *TCL1*. *Mol Cell Biol*. 2002;22(5):1513-1525.
- Shifera AS. Protein-protein interactions involving IKKgamma (NEMO) that promote the activation of NF- $\kappa$ B. *J Cell Physiol*. 2010;223(3):558-561.
- Thyss R, Virolle V, Imbert V, Peyron JF, Aberdam D, Virolle T. NF- $\kappa$ B/Egr-1/Gadd45 are sequentially activated upon UVB irradiation to mediate epidermal cell death. *EMBO J*. 2005;24(1):128-137.
- Pekarsky Y, Zanesi N, Aqeilan RI, Croce CM. Animal models for chronic lymphocytic leukemia. *J Cell Biochem*. 2007;100(5):1109-1118.
- Herling M, Patel KA, Teitell MA, et al. High *TCL1* expression and intact T-cell receptor signaling define a hyperproliferative subset of T-cell prolymphocytic leukemia. *Blood*. 2008;111(1):328-337.
- Ropars V, Despouy G, Stern MH, Benichou S, Roumestand C, Arold ST. The *TCL1A* oncoprotein interacts directly with the NF- $\kappa$ B inhibitor I $\kappa$ B. *PLoS One*. 2009;4(8):e6567.